Hindawi Publishing Corporation
Laser Chemistry
Volume 2008, Article ID 493059, 7 pages
doi:10.1155/2008/493059

Research Article

Two-Photon Polymerization of Hybrid Sol-Gel Materials for Photonics Applications

A. Ovsianikov,[1] A. Gaidukeviciute,[1] B. N. Chichkov,[1] M. Oubaha,[2] B. D. MacCraith,[2] I. Sakellari,[3,4] A. Giakoumaki,[3,5] D. Gray,[3] M. Vamvakaki,[3,5] M. Farsari,[3] and C. Fotakis[3,4]

[1] *The Laser Zentrum Hannover e.V., 30419 Hannover, Germany*
[2] *The Optical Sensors Laboratory, National Centre for Sensor Research, Dublin City University, Dublin 9, Ireland*
[3] *Institute of Electronic Structure and Laser, Foundation for Research and Technology - Hellas, P.O. Box 1527, 711 10 Heraklion, Greece*
[4] *Department of Physics, University of Crete, 71003 Heraklion, Crete, Greece*
[5] *Department of Materials Science and Technology, University of Crete, 710 03 Heraklion, Crete, Greece*

Correspondence should be addressed to B. N. Chichkov, b.chichkov@lzh.de

Received 24 April 2008; Accepted 12 July 2008

Recommended by Saulius Juodkazis

Two-photon polymerization of photosensitive materials has emerged as a very promising technique for the fabrication of photonic crystals and devices. We present our investigations into the structuring by two-photon polymerization of a new class of photosensitive sol-gel composites exhibiting ultra-low shrinkage. We particularly focus on two composites, the first containing a zirconium alkoxide and the second a nonlinear optical chromophore. The three-dimensional photonic crystal structures fabricated using these materials demonstrate high resolution and clear bandstops in the near IR region.

1. Introduction

Nonlinear optical stereolithography is a laser technique which allows the direct-writing of high-resolution three-dimensional (3D) structures. The technique is based on the two-photon polymerization (2PP) of photosensitive materials; when the beam of a femtosecond infrared laser is tightly focused within the volume of such a material, the polymerization process can be initiated by nonlinear absorption within the focal volume. By moving the laser focus through the resin in the three dimensions, 3D structures can be fabricated. A variety of acrylate [1–7] and epoxy [8, 9] materials have been used to make components and devices such as photonic crystals templates [10], mechanical devices [11, 12], plasmonic structures [13, 14], biomolecule scaffolds [15, 16], and microscopic models [17, 18]. The highest resolution reported to date is 65 nm [19].

The first materials employed in 2PP were acrylic photopolymers and the negative photoresist SU8 [8, 9, 18]; more recently, photosensitive sol-gel hybrid materials [20] such as the commercially available ORMOCER [21, 22] have been used. These materials benefit from straight-forward preparation, modification, and processing and in combination with their high optical quality, postprocessing chemical and electrochemical inertness, and good mechanical and chemical stability, they are emerging as a very useful class of materials for multiphoton polymerization [23]. The process is based on the phase transformation of a sol obtained from metallic oxide or alkoxide precursors. This sol is first hydrolyzed and condensed at a low temperature to form a wet gel. It is subsequently polymerized through radical photopolymerization to give a product similar to glass.

In this paper, we report our investigations into the structuring by two photon polymerization of two composite sol-gel materials. The first material is a zirconium/silicon composite; we show that by changing the zirconium/silicon ratio, we can tune the refractive index of the material. The second material is a copolymer of a photosensitive silicon alkoxide with a nonlinear optical (NLO) alkoxysilane; this is used to make 3D photonic crystals containing an NLO chromophore. These materials share the characteristic of minimal shrinkage during photopolymerization.

2. Experimental

2.1. Materials Synthesis and Preparation

A photosensitive sol-gel process usually involves the catalytic hydrolysis of sol-gel precursors and the heat-activated polycondensation of the hydrolyzed products followed by the photopolymerization of the organic moieties to form a macromolecular network structure of hybrid sol-gel materials. The material is generally formed through a 4-step process.

(1) The first step is the hydrolysis and condensation in which precursors or monomers such as metal oxides or metal alkoxides are mixed with water and then undergo hydrolysis and condensation to form a porous interconnected cluster structure. Either an acid such as HCl or a base like NH_3 can be employed as a catalyst.

(2) The second step includes gelation, where the solvent is removed and a gel is formed by heating at low temperature. Hydrolysis and condensation do not stop with gelation; it is at this stage that solvents are removed and any significant volume loss occurs.

(3) Thirdly, the process moves to photopolymerization. Because of the presence of the double bonds and provided that a photoinitiator has been added to the gel, the photoinduced radicals will cause polymerization only in the area in which they are present. At this step, there is no material removal and no volume loss; the reaction that occurs is the cleavage of the pendant carbon-carbon double bonds by a free-radical process to form the organic polymer backbone.

(4) Finally comes the development step; the sol-gel is immersed in an appropriate solvent and the area of the sol-gel that is not photopolymerized is removed.

In this work, the sol-gel process has been used to prepare two different photosensitive composites, a zirconium containing hybrid and an NLO hybrid. The synthesis of these materials is described below.

2.2. Zirconium Composite Synthesis

The material was fabricated from methacryloxypropyltrimethoxysilane (MAPTMS, Polysciences Inc.) and methacrylic acid (MAA, Sigma-Aldrich), both of which possess photopolymerizable methacrylate moieties. Zirconium n-propoxide $Zr(OPr)_4$, (ZPO, 70% solution in 1-propanol, Sigma-Aldrich) was used as an inorganic network former. The molar ratio of MAPTMS to ZPO was varied from 10 : 0 to 5 : 5, in order to investigate the processability and the refractive index variation of the resulting copolymer.

MAPTMS was firstly hydrolyzed by adding HCl, (concentration 0.01 M) at a 1 : 0.75 ratio and the mixture was stirred for 30 minutes. ZPO was chelated by adding MAA (molar ratio ZPO:MAA, 1 : 1), an equal volume of 1-PrOH was then added, and the sol was stirred for 30 minutes. The MAPTMS sol was added drop-wise to the stirred ZPO sol. Following another 45 minutes, water was added to this mixture with a final 2.5 : 5 MAPTMS:H_2O molar ratio. 4,4′-Bis(diethylamino)benzophenone (Sigma-Aldrich), 1% to the final product was used as a photoinitiator (PI). The photoinitiator Irgacure 369 was obtained from Ciba Speciality Chemicals. After stirring for 24 hours, the materials were filtered using 0.22 μm filters.

The samples were prepared by spin-coating or drop-casting onto glass substrates, and the resultant films were dried on a hotplate at 100°C for 1 hour before the photopolymerization. The heating process resulted in the condensation of the hydroxy-mineral moieties and the formation of the inorganic matrix. In a subsequent processing step, the material, which was not exposed to the laser radiation, was removed by developing in 1-propanol (Sigma-Aldrich).

The transmission spectra of thin films of this material were measured using a UV-Vis (Perkin-Elmer) spectrometer. Thin films were prepared by spin-coating and drying on a hotplate at 100°C for 1 hour. Figure 1 shows the difference in the absorption spectra induced by the addition of ZPO and photoinitiator. It can be seen that in the presence of photoinitiator even the addition of only 1% ZPO causes the absorption region to extend from 420 nm to 500 nm. A further increase in the amount of ZPO also causes an increase of the absorption around 470 nm; however, as also reported by Bhuian et al. [23], the extension of the absorption band disappears when no PI is added to the sol-gel composite; it also disappears when the composite is in solution. This behavior indicates an interaction between the ZPO and the PI which requires molecular proximity; a possible explanation is a charge transfer between the two composites.

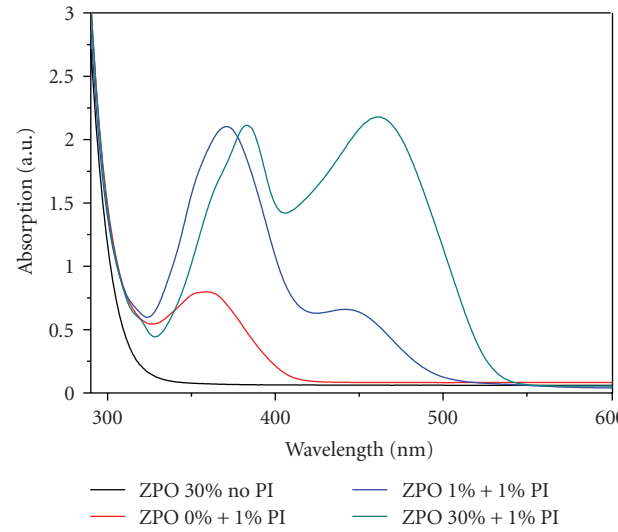

Figure 1: Transmission spectra for the material with varying ZPO and photoinitiator (PI) content. PI alone results in absorption around 360 nm. Addition of PI to ZPO containing material extends the absorption region from 420 nm to 500 nm.

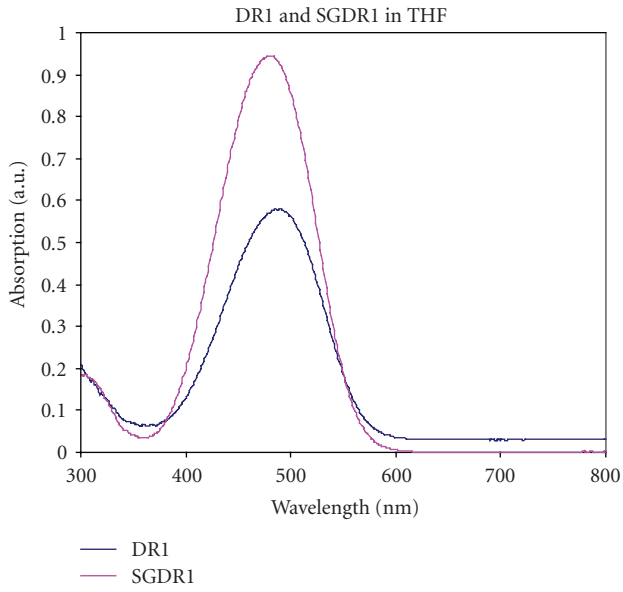

Figure 2: Absorption spectrum of DR1 and SGDR1 in THF.

2.3. NLO Hybrid Synthesis

The second material prepared consisted of the second-order NLO chromophore DR1 (Disperse Red 1, Sigma-Aldrich), which was firstly reacted with (3-isocyanatopropyl) triethoxysilane to form a functionalized silicon alkoxide precursor (SGDR1); SGDR1 was subsequently mixed with MAPTMS and the PI.

(3-isocyanatopropyl) trimethoxysilane and dibutyltin dilaurate (DBTDL) were purchased from Sigma-Aldrich and used without further purification. DR1 was recrystallized twice from ethanol before use. The synthesis of the NLO-active triethoxysilane was carried out according to [24]. (3-isocyanatopropyl) trimethoxysilane and DR1 at a 2 : 1 mole ratio were dissolved in anhydrous tetrahydrofuran (THF) under a nitrogen atmosphere. Next, 1 wt% DBTDL was added to the reaction flask and the solution was refluxed for 4 hours. The resultant solution was reduced to about half its initial volume under vacuum, followed by precipitation of the product as a red solid in hexane. The final product (SGDR1) was dried in a vacuum oven at 60°C for 24 hours and subsequently stored under vacuum until use. The product was characterized by ^{1}H NMR spectroscopy which verified the successful synthesis of SGDR1.

To obtain the photosensitive gel, SGDR1 was first dissolved in toluene and stirred for 24 hours. Then MAPTMS was added to the SGDR1 solution (SGDR1 up to 40% w/w) and the mixture was hydrolyzed by the addition of HCl (pH = 1). After stirring for 1 hour, Irgacure 369 (up to 3.3 wt% to MAPTMS) was added and the mixture was stirred for a further 1 hour. To remove any aggregates, the solution was filtered through a 0.22 μm pore size Millipore syringe filter. After filtration, the solution remained clear without any sign of further particle aggregation for several weeks. Thermogravimetric analysis of the composite showed that it was stable up to 250°C, above which temperature it started to decompose.

The absorption spectra of both DR1 and SGDR1 are shown in Figure 2. Due to the presence of the DR1 azobenzene rings, the composite material absorbs very strongly in the spectral region 400–550 nm, but it is completely transparent at 600–800 nm and has a window of transparency in the spectral region 300–400 nm. These properties make SGDR1 ideal for two-photon polymerization using a Ti:Sapphire laser. The IR transparency allows focusing the laser within the volume of the material, while the relatively high UV transparency means that there will be two-photon absorption mostly by the PI, and not by the NLO chromophore.

Films were prepared by drop-casting the above mixture on 100 μm thick glass substrates, and the resultant films were baked at 100°C for 1 hour, to condense the silanol moieties and remove any residual solvent. After the completion of the photopolymerization process, the sample was developed for three minutes in THF and rinsed in isopropanol.

3. Experimental Techniques

Refractive Index Measurements

The refractive index of the sol-gel films at 632.8 nm was determined from an m-line prism coupling experiment [25], using He-Ne laser. A thin film of the material was first made by spin-coating and subsequent curing under a UV lamp. A Schott Glass SF6 prism, as a higher refractive index medium, was used to couple light into the TE modes of the material waveguide; the sample was then mounted on a high-resolution rotation stage. The laser beam was directed toward the sample, and the transmitted light was detected with a photodiode. The coupling angles were then determined, and from the prism angle and refractive index the mode could then be determined. From the crossing point of the modes supported by the thin film, both the thickness and the refractive index of the film could be then calculated, using the mode equation [16, 26].

4. 3D Microfabrication by Two-Photon Polymerization

The experimental setup for the fabrication of three-dimensional microstructures by two-photon polymerization is shown in Figure 3. In the present work, two different Ti:Sapphire femtosecond lasers were used; for the processing of the MAPTMS:SGDR1 composite, the laser characteristics were 60 fs, 90 MHz, <450 mW, 780 nm, while for the MAPTMS:ZPO composite, it was 140 fs, 80 MHz, 780 nm. A 100X microscope objective lens (Zeiss, Plan Apochromat, N.A. = 1.4) was used to focus the laser beam into the volume of the photosensitive material. The photopolymerized structure was generated in a layer-by-layer format, by using an x-y galvanometric mirror scanner. Movement on the z-axis was achieved using a high resolution linear stage.

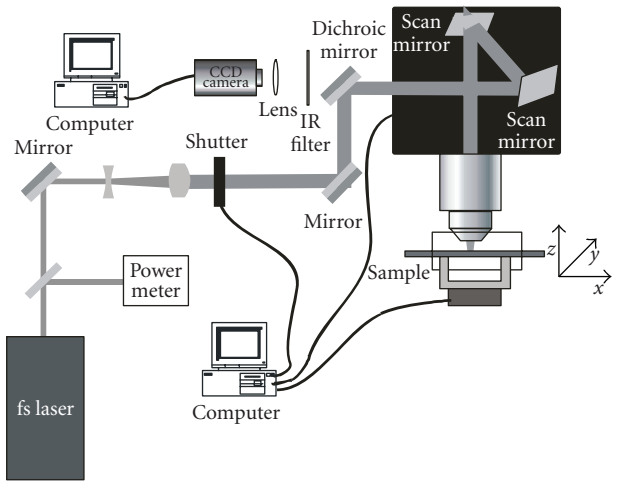

Figure 3: Experimental setup for two-photon polymerization.

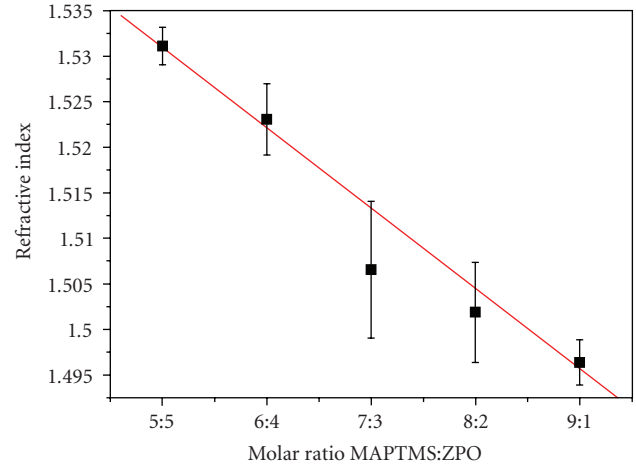

Figure 4: Refractive index variation of the MAPTMS:ZPO complex.

For the online monitoring of the photopolymerization process, a CCD camera was mounted behind a dichroic mirror. As the refractive index of the photopolymer changes during polymerization, the illuminated structure becomes visible during the building process.

5. Results

Refractive Index Measurements

In the case of the MAPTMS:SGDR1 composite, the refractive index of the material was measured for 10% w/w SGDR1 content and was found to be $n = 1.497 \pm 0.006$.

In the case of the zirconium-containing sol-gel, by varying the molar ratio of MAPTMS and ZPO, the refractive index of the composite could be modified (Figure 4). It can be seen that as the ZPO content increases, so does the material's refractive index. The fact that this increase is linear greatly simplifies the material design criteria, as typically such increases are saturating so that the doping concentration becomes very critical. However, in this concentration range, no such limitation is apparent.

6. Two-Photon Fabrication of Photonic Crystals

For the fabrication of the photonic crystals, the woodpile geometry was chosen. It consists of layers of one-dimensional rods with a stacking sequence that repeats itself every four layers. The distance between four adjacent layers is "a" and within each layer, the axes of the rods are parallel to each other with a distance "d" between them. The adjacent layers are rotated by 90°. Between every other layer, the rods are shifted relative to each other by "$d/2$." For the case of "a/d" $= \sqrt{2}$, the lattice can be derived from a face-centred-cubic (fcc) unit cell with a basis of two rods. A constant "a/d" ratio of 1.34 was applied for all the woodpile structures presented here.

SGDR1 Photonic Crystals

Photonic crystals are considered to be an optical equivalent of semiconductors, since they modify the properties of light in the same way as semiconductors do for electrons. However, in contrast to electrons, photon energy cannot be easily tuned. Therefore, fabrication of photonic crystals made of nonlinear materials, whose optical response depends on propagating light intensity, is important.

Figure 5(a) shows a microscope image of an array of photonic crystals; they have the bright red color of Disperse Red 1. Figure 5(b) shows a scanning electron microscope (SEM) image of a DR1-containing photonic crystal fabricated by the 2PP method using a laser fluence of 44 mJ/cm^2 and a beam scanning speed of 20 μm/s. As it can be seen, SGDR1 can be structured very accurately and without defects. The smallest lateral feature size that was experimentally obtained with this material is 250 nm. The refractive index of the material was found to be $n = 1.497 \pm 0.006$ (10% w/w SGDR1 content).

ZPO Photonic Crystals

Figure 6 shows one of the fabricated woodpile photonic crystal structures exhibiting a bandstop in the near-IR region; in this case, the employed material had an 8 : 2 MAPTMS:ZPO molar ratio. As the material exhibits negligible distortion due to photopolymerization, no additional efforts such as precompensation or mechanical stabilization to avoid structural distortions are necessary.

FTIR measurements (Equinox, Bruker Optics) of the reflection and the transmission spectra of woodpile structures with rod distances between 1.2 μm and 1.8 μm indicate clear bandstops with the central frequency shifting to shorter wavelengths as the rod distance is reduced (see Figure 7). In addition, the spectra show the appearance of higher order bandstops in all samples, indicating the high quality of the fabricated structures. The observed bandstop positions are blue shifted when compared to the values estimated from

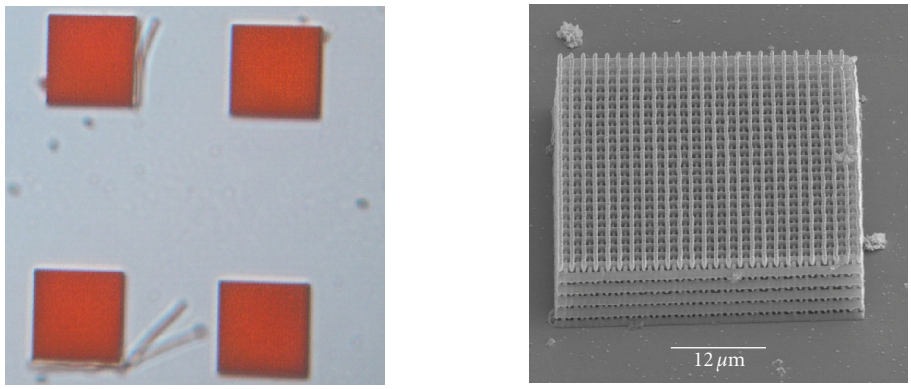

(a) (b)

Figure 5: Optical microscope (a) and SEM (b) images of photonic crystals by MAPTMS:SGDR1.

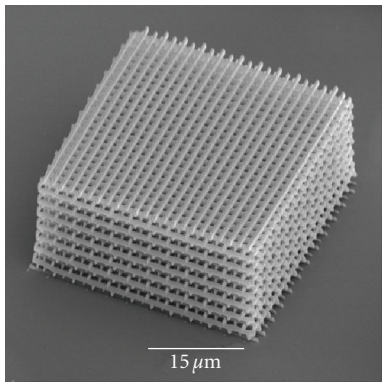

Figure 6: SEM image of Zr-containing photonic crystal structure (applied material MAPTMS:ZPO ratio is 8 : 2).

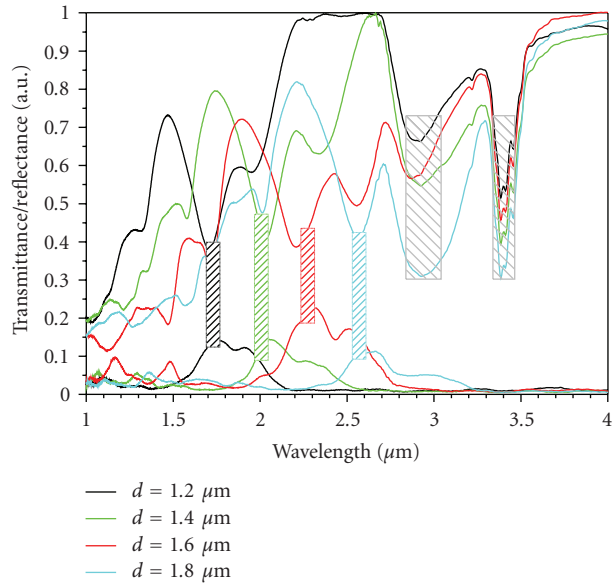

Figure 7: FTIR spectra of zirconium-containing photonic crystal structures with rod spacings 1.2 μm–1.8 μm (applied material MAPTMS:ZPO ratio is 8 : 2).

Bragg's condition or obtained from theoretical simulations. There are two additional bands at 3 μm and 3.4 μm whose origin is the absorption of the material, as confirmed by measurements of transmission through flat, unstructured layers. Also in this case, material with 8 : 2 MAPTMS:ZPO molar ratio was used. The material has no natural absorption in the spectral region 550–2700 nm, which makes it suitable for structuring by 2PP using a 780 nm laser and for making photonic crystal structures at telecommunication wavelengths.

The observed splitting of the absorption and transmission peaks as well as blue shift of the bandstops central position can be explained by taking a closer look at the experimental setup used for the FTIR transmission measurements. In order to focus the beam on the size of the fabricated photonic crystal, a Cassegrain reflective optical assembly is used. In contrast to the ideal case, when the measuring beam is perpendicular to the surface of the structure, this assembly provides illumination of the structure with a hollow light cone having an acceptance angle between 15° and 30°. Previous studies on 3D photonic crystal systems have shown that scattering of the measuring beam entering the photonic crystal at a large angle leads to the reflection peak splitting and a blue shift of its central position [27–29] Theoretical simulations have also confirmed these observations [30].

An approach taken by many groups is the templating of photonic crystals by inversion, infiltrating them with another, higher refractive index material [8, 18]. The materials described here also can be used for template fabrication. Like most hybrids, their organic components decompose at relatively low temperatures (approx. 220°C). The inorganic components, however, which are dominant after condensation in the materials described here, are very resistant to high temperatures. It should be possible to remove them by HF acid, in order to obtain the inverse structures, as has been demonstrated in similar material systems [31].

7. Conclusions

We have presented our investigations into two sol-gel hybrid photosensitive materials which can be structured accurately by two-photon polymerization. The first is a zirconium containing sol-gel; by varying its zirconium content, we have shown it is possible to "tune" its refractive index. The second material contains the nonlinear optical chromophore Disperse Red 1; it is a first step towards the fabrication of nonlinear three-dimensional photonic crystal devices using the two-photon polymerization technique.

As neither materials shrinks during photopolymerization, it was possible to fabricate photonic crystals with bandstops in the near IR region without any precompensation for structure distortions induced by the material shrinkage, or any support structures for their mechanical stabilization.

Acknowledgments

This work was supported by the Marie Curie Transfer of Knowledge project "NOLIMBA" (MTKD-CT-2005-029194) and by the UV Laser Facility operating at IESL-FORTH under the European Commission "Improving Human Research Potential" program (RII3-CT-2003-506350). The authors would like to thank group of Professor Martin Wegener for valuable assistance in optical characterisation of photonic crystals. Travel between Crete, Greece and Hannover, Germany, was supported by an IKYDA/DAAD travel grant.

References

[1] S. Maruo, O. Nakamura, and S. Kawata, "Three-dimensional microfabrication with two-photon-absorbed photopolymerization," *Optics Letters*, vol. 22, no. 2, pp. 132–134, 1997.

[2] S. Kawata, H.-B. Sun, T. Tanaka, and K. Takada, "Finer features for functional microdevices," *Nature*, vol. 412, no. 6848, pp. 697–698, 2001.

[3] X.-M. Duan, H.-B. Sun, K. Kaneko, and S. Kawata, "Two-photon polymerization of metal ions doped acrylate monomers and oligomers for three-dimensional structure fabrication," *Thin Solid Films*, vol. 453-454, pp. 518–521, 2004.

[4] D. McPhail, M. Straub, and M. Gu, "Optical tuning of three-dimensional photonic crystals fabricated by femtosecond direct writing," *Applied Physics Letters*, vol. 87, no. 9, Article ID 091117, 3 pages, 2005.

[5] L. H. Nguyen, M. Straub, and M. Gu, "Acrylate-based photopolymer for two-photon microfabrication and photonic applications," *Advanced Functional Materials*, vol. 15, no. 2, pp. 209–216, 2005.

[6] M. Straub and M. Gu, "Near-infrared photonic crystals with higher-order bandgaps generated by two-photon photopolymerization," *Optics Letters*, vol. 27, no. 20, pp. 1824–1826, 2002.

[7] S. H. Wu, M. Straub, and M. Gu, "Single-monomer acrylate-based resin for three-dimensional photonic crystal fabrication," *Polymer*, vol. 46, no. 23, pp. 10246–10255, 2005.

[8] M. Deubel, G. von Freymann, M. Wegener, S. Pereira, K. Busch, and C. M. Soukoulis, "Direct laser writing of three-dimensional photonic-crystal templates for telecommunications," *Nature Materials*, vol. 3, no. 7, pp. 444–447, 2004.

[9] T. Kondo, S. Matsuo, S. Juodkazis, V. Mizeikis, and H. Misawa, "Multiphoton fabrication of periodic structures by multibeam interference of femtosecond pulses," *Applied Physics Letters*, vol. 82, no. 17, pp. 2758–2760, 2003.

[10] H.-B. Sun, S. Matsuo, and H. Misawa, "Three-dimensional photonic crystal structures achieved with two-photon-absorption photopolymerization of resin," *Applied Physics Letters*, vol. 74, no. 6, pp. 786–788, 1999.

[11] P. Galajda and P. Ormos, "Complex micromachines produced and driven by light," *Applied Physics Letters*, vol. 78, no. 2, pp. 249–251, 2001.

[12] H.-B. Sun, K. Takada, and S. Kawata, "Elastic force analysis of functional polymer submicron oscillators," *Applied Physics Letters*, vol. 79, no. 19, pp. 3173–3175, 2001.

[13] R. Kiyan, C. Reinhardt, S. Passinger, et al., "Rapid prototyping of optical components for surface plasmon polaritons," *Optics Express*, vol. 15, no. 7, pp. 4205–4215, 2007.

[14] C. Reinhardt, S. Passinger, B. N. Chichkov, C. Marquart, I. P. Radko, and S. I. Bozhevolnyi, "Laser-fabricated dielectric optical components for surface plasmon polaritons," *Optics Letters*, vol. 31, no. 9, pp. 1307–1309, 2006.

[15] R. J. Narayan, C. Jin, A. Doraiswamy, et al., "Laser processing of advanced bioceramics," *Advanced Engineering Materials*, vol. 7, no. 12, pp. 1083–1098, 2005.

[16] R. J. Narayan, C. Jin, T. Patz, et al., "Laser processing of advanced biomaterials," *Advanced Materials & Processes*, vol. 163, no. 4, pp. 39–42, 2005.

[17] M. Straub, L. H. Nguyen, A. Fazlic, and M. Gu, "Complex-shaped three-dimensional microstructures and photonic crystals generated in a polysiloxane polymer by two-photon microstereolithography," *Optical Materials*, vol. 27, no. 3, pp. 359–364, 2004.

[18] J. Serbin, A. Ovsianikov, and B. N. Chichkov, "Fabrication of woodpile structures by two-photon polymerization and investigation of their optical properties," *Optics Express*, vol. 12, no. 21, pp. 5221–5228, 2004.

[19] W. Haske, V. W. Chen, J. M. Hales, et al., "65 nm feature sizes using visible wavelength 3-D multiphoton lithography," *Optics Express*, vol. 15, no. 6, pp. 3426–3436, 2007.

[20] A.-L. Pénard, T. Gacoin, and J.-P. Boilot, "Functionalized sol-gel coatings for optical applications," *Accounts of Chemical Research*, vol. 40, no. 9, pp. 895–902, 2007.

[21] R. Houbertz, L. Fröhlich, M. Popall, et al., "Inorganic-organic hybrid polymers for information technology: from planar technology to 3D nanostructures," *Advanced Engineering Materials*, vol. 5, no. 8, pp. 551–555, 2003.

[22] J. Serbin, A. Egbert, A. Ostendorf, et al., "Femtosecond laser-induced two-photon polymerization of inorganic organic hybrid materials for applications in photonics," *Optics Letters*, vol. 28, no. 5, pp. 301–303, 2003.

[23] B. Bhuian, R. J. Winfield, S. O'Brien, and G. M. Crean, "Investigation of the two-photon polymerisation of a Zr-based inorganic-organic hybrid material system," *Applied Surface Science*, vol. 252, no. 13, pp. 4845–4849, 2006.

[24] D. H. Choi, J. H. Park, T. H. Rhee, N. Kim, and S.-D. Lee, "Improved temporal stability of the second-order nonlinear optical effect in a sol-gel matrix bearing an active chromophore," *Chemistry of Materials*, vol. 10, no. 3, pp. 705–709, 1998.

[25] S. Monneret, P. Huguet-Chantôme, and F. Flory, "m-lines technique: prism coupling measurement and discussion of accuracy for homogeneous waveguides," *Journal of Optics A*, vol. 2, no. 3, pp. 188–195, 2000.

[26] P. K. Tien, G. Smolinsky, and R. J. Martin, "Thin organosilicon films for integrated optics," *Applied Optics*, vol. 11, no. 3, pp. 637–642, 1972.

[27] S. G. Romanov, T. Maka, C. M. S. Torres, et al., "Diffraction of light from thin-film polymethylmethacrylate opaline photonic crystals," *Physical Review E*, vol. 63, no. 5, Article ID 056603, 5 pages, 2001.

[28] S. G. Romanov, M. Bardosova, D. E. Whitehead, I. M. Povey, M. Pemble, and C. M. S. Torres, "Erasing diffraction orders: opal versus Langmuir-Blodgett colloidal crystals," *Applied Physics Letters*, vol. 90, no. 13, Article ID 133101, 3 pages, 2007.

[29] M. Deubel, M. Wegener, S. Linden, and G. von Freymann, "Angle-resolved transmission spectroscopy of three-dimensional photonic crystals fabricated by direct laser writing," *Applied Physics Letters*, vol. 87, no. 22, Article ID 221104, 3 pages, 2005.

[30] A. V. Lavrinenko and S. G. Romanov, "The finite-difference time-domain modeling of bi-directional transmission spectra in thin 3-dimensional opal-based photonic crystals," in *Proceedings of the International Symposium on Photonic and Electromagnetic Crystal Structures (PECS '07)*, Monterey, Calif, USA, April 2007.

[31] Y. Jun, P. Nagpal, and D. J. Norris, "Thermally stable organic-inorganic hybrid photoresists for fabrication of photonic band gap structures with direct laser writing," *Advanced Materials*, vol. 20, no. 3, pp. 606–610, 2008.